Article

Zheshengite, $Pb_4ZnZn_2(AsO_4)_2(PO_4)_2(OH)_2$: A New Mineral of the Dongchuanite Group and the Influence of As–P Isomorphic Substitution on Unit-Cell Parameters of Dongchuanite Group Minerals

Ningyue Sun [1], Guowu Li [1,*], Yuan Xue [1], Hongtao Shen [2] and Jinhua Hao [1]

1 Science Research Institute, China University of Geosciences, Beijing 100083, China; sunningyue1998@163.com (N.S.); xue.yuea@163.com (Y.X.); haojh@cugb.edu.cn (J.H.)
2 State Key Laboratory of Geological Processes and Mineral Resources, China University of Geosciences, Wuhan 430074, China; aurevoir_bonsoir@foxmail.com
* Correspondence: liguowu@cugb.edu.cn

Abstract: Zheshengite (IMA2022-011), $Pb_4ZnZn_2(AsO_4)_2(PO_4)_2(OH)_2$, is a new mineral from Sanguozhuang Village in the eastern Dongchuan Copper Ore Field, Yunnan Province, China. The new mineral is named after Zhesheng Ma (1937–). Zheshengite occurs as prismatic single crystals with chisel-like terminations on hemimorphite, with crystal sizes ranging from 0.02 to 0.05 mm. It is a brittle mineral with irregular fractures, a Mohs hardness of 2½ to 3, perfect cleavage on {011}, and a calculated density of 6.26 g/cm³. The empirical formula of zheshengite, based on 18 O atoms per formula unit, is $(Pb_{4.12}Ca_{0.01})_{\sum 4.13}(Zn_{0.83}Cu_{0.23}Fe_{0.04})_{\sum 1.10}Zn_{2.00}[(As_{0.90}P_{0.10})_{\sum 1.00}O_4]_2[(P_{0.94}Si_{0.01})_{\sum 0.95}O_4]_2(OH)_2$. Zheshengite exhibits a triclinic structure (space group $P-1$, no. 2), with unit-cell parameters: $a = 4.7746(4)$ Å, $b = 8.4920(7)$ Å, $c = 10.4056(8)$ Å, $\alpha = 97.087(7)°$, $\beta = 101.060(7)°$, $\gamma = 92.996(7)°$, $V = 409.66(6)$ Å³, and $Z = 1$. As a member of the dongchuanite group, zheshengite features a dongchuanite-type structure. This study reveals the impact of As–P isomorphic substitution on unit-cell parameters in the dongchuanite group, identifying correlations between As content and changes in parameters a and V, which may serve as diagnostic indicators for dongchuanite group minerals. In addition, the structure studies of zheshengite may have implications for environmental protection.

Keywords: new mineral; zheshengite; crystal structure; unit-cell parameters; As–P isomorphic substitution; dongchuanite group

1. Introduction

Zheshengite (IMA2022-011) is a new mineral approved by the International Mineralogical Association's Commission on New Minerals, Nomenclature and Classification (IMA-CNMNC) and designated with the symbol "Zh". It belongs to the dongchuanite group, which is also approved by IMA-CNMNC [1]. A different root name was selected for zheshengite because the ideal formula of dongchuanite contains only $(PO_4)^{3-}$ anions, whereas zheshengite's formula includes both $(PO_4)^{3-}$ and $(AsO_4)^{3-}$ anions. Zheshengite is named in honor of Chinese mineralogist Zhesheng Ma (born 1937), a former professor at the China University of Geosciences (Beijing). She conducted extensive mineralogical research in the Dongchuan Copper ore field and was the first to describe tangdanite (formerly known as "clinotyrolite"), a new mineral discovered in that region.

The dongchuanite group minerals typically contain Pb, Zn, Cu, As, and P, exhibiting a unique elemental combination that has not been reported in other IMA-CNMNC approved minerals or synthetic compounds. Among these elements, Pb, Zn, and Cu are common environmentally hazardous heavy metals that are often exposed to the environment through human mining activities [2]. These metals may migrate into water and soil, causing negative

environmental impacts, including soil degradation, the loss of organic matter, the alteration of soil physical structure, and heavy metal contaminations of water bodies [3,4].

Arsenic (As), also a toxic element, can pollute drinking water through mining activities [5,6]. Prolonged exposure to arsenic-contaminated water can lead to arsenic poisoning, posing severe health risks. Accordingly, the World Health Organization (WHO) recommends a limit of 10 µg/L arsenic in drinking water [7]. In addition, the accumulation of arsenic in soil inhibits plant growth, disrupts ecosystems, and can enter the food chain through crops, threatening human health [8].

Dongchuan has a long history of mining, and the environmental pollution associated with mining activities cannot be overlooked. With their novel crystal structures and chemical compositions, dongchuanite group minerals can potentially immobilize multiple environmentally harmful elements within their crystal lattices. A deeper understanding of their crystal structures may offer valuable applications for environmental protection.

The presence of multiple crystallographic sites leads to complex and interesting crystallographic phenomena within the dongchuanite group mineral. In the descriptive studies on dongchuanite group minerals, we aim to explore their crystal structure and chemistry from various perspectives. A previous study on dongchuanite provides general information of the crystal structure and chemistry of the dongchuanite mineral group [9]. Simultaneously, in an article dedicated to cuprozheshengite, there is evidence for the ordered distribution of As-P atoms at $X1$ and $X2$ site [10]. The cuprodongchuanite study primarily focuses on atomic occupancy at the B sites and the Jahn–Teller effect (publication pending). In this paper, we provide a detailed description of the new mineral, zheshengite. Additionally, we discuss the influence of As-P isomorphous substitution on the cell parameters of the dongchuanite group.

The zheshengite holotype specimen is deposited at the Geological Museum of China, Xisi Yangrou Hutong No. 15, Xicheng District, Beijing, China (catalog no. M16134). A co-type specimen is kept in the Crystal Structure Laboratory at China University of Geosciences, Beijing, China (catalog no. DC-5).

2. Occurrence and Associated Minerals

Zheshengite was first discovered in Sanguozhuang Village, located in the eastern part of the Dongchuan Copper Ore Field, Dongchuan District, Kunming City, Yunnan Province, China (26°8′14″ N, 102°59′36″ E). This ore field, one of China's most significant copper deposits, has been crucial for copper production and coin minting since the Tang Dynasty (618–907 CE) [11]. Its significance was particularly notable during the Qing Dynasty (1644–1912 CE) [12]. The area is characterized by sedimentary rock-hosted, strata-bound copper deposits [13,14], with predominantly disseminated and veinlet copper sulfides [15].

The zheshengite samples were collected from an abandoned mine at over 3000 m in elevation, approximately 1.7 km northwest of Sanguozhuang Village. The site first attracted attention when local miners discovered high-quality veszelyite, drawing interest from mineral collectors. Zheshengite was located within the heavily weathered zone of a mineral vein hosted in dolomite. The vein is composed of tennantite-(Zn), sphalerite, galena, and minor pyrite as the primary minerals, with quartz serving as the main gangue mineral. Numerous secondary minerals have formed in voids created by the weathering of primary minerals, suggesting a supergene origin. In addition to dongchuanite group minerals, the area contains a variety of other supergene minerals, including arsenoveszelyite, arsendescloizite, bayldonite, duftite, hemimorphite, kipushite, theisite, and veszelyite, all contributing to the mineralogical diversity of the region.

3. Analytical Methods

3.1. Chemical Composition Analysis

The quantitative chemical composition of zheshengite was analyzed at the Electron Probe Micro-Analysis Lab, China University of Geosciences (Beijing, China), using a Shimadzu EPMA-1720 (Electron Probe Micro-Analyzer) equipped with a wavelength

dispersive spectrometer (WDS). The operating conditions were 15 kV of accelerating voltage, a 10 nA beam current, and a 5 μm beam diameter. Standards used are listed in Table 1.

Table 1. The chemical composition of zheshengite (wt.%) obtained from EPMA analysis.

Constituent	Mean	Range	S.D. (σ) [1]	Reference Material
V_2O_5	0.02	0–0.07	0.02	Vanadium
SiO_2	0.07	0.03–0.12	0.03	Sanidine
CuO	1.20	0.10–2.02	0.59	Chalcopyrite
As_2O_5	13.50	11.34–14.59	0.73	Cobaltite
FeO [2]	0.19	0.04–0.41	0.09	Garnet
P_2O_5	9.54	8.67–10.99	0.58	Apatite
ZnO	14.95	13.65–16.75	0.94	Willemite
PbO	59.75	59.34–60.34	0.40	Crocoite
CaO	0.05	0.03–0.08	0.02	Apatite
H_2O [3]	1.17			
Total	100.44			

[1] S.D.—standard deviation. [2] Total Fe content and valence of iron are not measured. [3] Calculated from crystal structure refinement.

3.2. Raman Spectrum Analysis

The Raman spectrum of zheshengite was recorded with a HORIBA LabRAM HR Evolution Raman spectrometer (532 nm laser with a power of 17 mW, equipped with a 600 gr/mm diffraction grating) via Reflex reflection mode. Data from 4000 to 200 cm^{-1} were collected with a 20 s acquisition, 2 scans, and 4 cm^{-1} resolution. The raw Raman data can be found in the supplementary materials.

3.3. Crystal Structure Analysis

The powder diffraction measurement was conducted with a Rigaku XtaLAB PRO-007HF diffractometer, utilizing a rotating crystal method. The instrument featured a rotating anode Mo$K\alpha$ X-ray source operating at 50 kV and 24 mA, paired with a hybrid pixel array detector. Powder diffraction cell parameters were refined using Chekcell software [16], while Vesta software [17] was used to calculate powder diffraction data.

Single-crystal X-ray diffraction analysis was also conducted on the same diffractometer, using a high-quality crystal fragment (0.010 mm × 0.020 mm × 0.030 mm) to capture hemisphere data ($-5 < h < 5$, $-10 < k < 10$, $-12 < l < 12$) with $R_{int} = 0.022$. Intensity data were corrected for Lorentz polarization and multi-scan absorption effects. Crystal structure determination and refinement were carried out with OLEX2-1.3 [18] using SHELXT [19]. The structure was solved by intrinsic phasing and refined to $R = 0.036$, based on 1315 independent reflections where $I > 2\sigma(I)$. Structure refinements confirmed the centrosymmetric space group $P-1$ (no. 2). Crystal structure data are available in the CIF file in the Online Materials.

3.4. Mineral Mapping

Mineral mapping was performed using a TESCAN Integrated Mineral Analyzer (TIMA) hosted at Kuangpu Geological Exploration Technology Co., Ltd., Xi'an, China. The instrument, a TESCAN MIRA3 Schottky field emission SEM, is equipped with energy-dispersive spectrometry (EDS) and software for automated quantitative mineralogical analysis. Analyses were conducted with a 25 kV, 10 nA electron beam at a 180 nm spot size and a 15 mm working distance. Calibration involved a Faraday cup for current and backscattered electrons (BSE) signals and a Mn standard for the EDS signal. Mineral identification was based on matching EDS spectra to a built-in database, with false-color mapping used to represent the spatial distribution of mineral phases.

4. Results

4.1. Appearance, Physical and Optical Properties

Unlike other dongchuanite group minerals, which typically form spherical aggregates, zheshengite occurs as prismatic single crystals with chisel-like termination. The size of single crystal ranges from 0.02 to 0.05 mm (Figure 1). The crystals are light yellow with a white streak. The crystals are translucent with a vitreous luster, brittle, and exhibit an irregular fracture. Notably, they show good cleavage, parallel to the {011} plane.
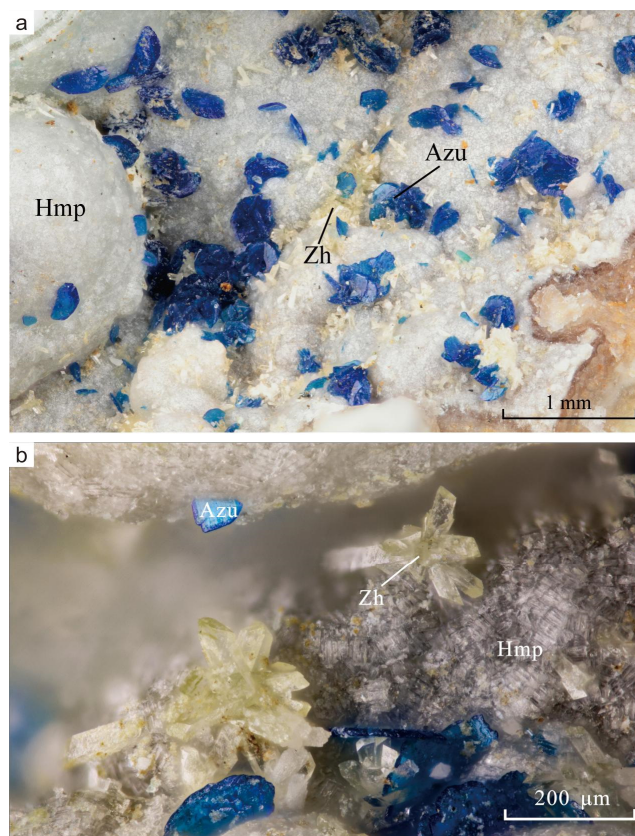

Figure 1. (**a**) Prismatic single crystals of zheshengite (Zh) associated with hemimorphite (Hmp) and azurite (Azu). (**b**) A closer view of zheshengite.

The small sample size prevented direct measurements of the mineral's density. From the empirical formula and unit-cell parameters obtained by single-crystal X-ray diffraction, the calculated density is 6.26 g/cm^3. The Mohs hardness of zheshengite is approximately 2½–3. This mineral dissolves in hydrochloric acid, producing white $PbCl_2$.

The mineral's refractive index (RI) exceeds that of the highest refractive oil typically used in measurements. The average refraction index, calculated using the Gladstone–Dale relationship [20], is 1.93.

4.2. Raman Spectrum

The Raman spectrum of zheshengite, shown in Figure 2, spans the range of 200–4000 cm^{-1}. Bands below 400 cm^{-1}, specifically at 375, 308, and 236 cm^{-1}, were assigned to lattice vibrations. The band at 422 cm^{-1} likely corresponds to the symmetric stretching mode of the ZnO_4 tetrahedron [21].
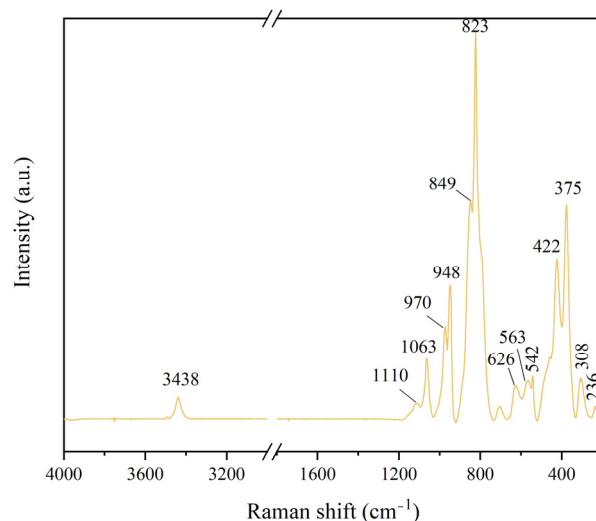
Figure 2. The Raman spectrum of zheshengite.

Bands between 650 and 450 cm^{-1} are attributed to the bending vibrations of PO$_4$ and AsO$_4$ tetrahedra. A weak feature at 626 cm^{-1} corresponds to the v_2 mode of (PO$_4$)$^{3-}$, while bands between 600 and 450 cm^{-1} are associated with v_4 or v_2 modes of (PO$_4$)$^{3-}$ and (AsO$_4$)$^{3-}$, including peaks at 563 and 542 cm^{-1} [22–24].

Bands in the range of 1100–650 cm^{-1} are attributed to the stretching vibrations of (PO$_4$)$^{3-}$ and (AsO$_4$)$^{3-}$ [25]. Two groups of split peaks related to (PO$_4$)$^{3-}$ were identified as the v_3 mode (1110, 1063 cm^{-1}) and the v_1 mode (970, 948 cm^{-1}), respectively. The peak at 823 cm^{-1}, with a shoulder at 849 cm^{-1}, corresponds to the v_3 mode of (AsO$_4$)$^{3-}$.

The sharp band at 3438 cm^{-1} indicates O–H stretching, confirming the presence of the OH$^-$ group [26].

4.3. Chemical Composition

The chemical composition data for zheshengite are presented in Table 1. Ten quantitative chemical data were obtained for zheshengite. The H$_2$O content was not directly determined. Crystal structure refinement and bond valence sum (BVS) analysis indicate that O9 is the single site for OH$^-$. The H$_2$O content is then calculated with the assumption of full OH$^-$ occupancy at the O9 site. Based on EPMA analysis and crystal structure refinement, the empirical formula is (Pb$_{4.12}$Ca$_{0.01}$)$_{\sum 4.13}$(Zn$_{0.83}$Cu$_{0.23}$Fe$_{0.04}$)$_{\sum 1.10}$Zn$_{2.00}$[(As$_{0.90}$P$_{0.10}$)$_{\sum 1.00}$O$_4$]$_2$[(P$_{0.94}$Si$_{0.01}$)$_{\sum 0.95}$O$_4$]$_2$(OH)$_2$, calculated with O = 18 *apfu*. The simplified formula is Pb$_4$(Zn,Cu)Zn$_2$[(As,P)O$_4$]$_2$[PO$_4$]$_2$(OH)$_2$, and the ideal formula is Pb$_4$ZnZn$_2$(AsO$_4$)$_2$(PO$_4$)$_2$(OH)$_2$, which requires PbO 58.48, ZnO 15.99, P$_2$O$_5$ 9.30, As$_2$O$_5$ 15.05, H$_2$O 1.18, total 100 wt.%.

The recommended Dana classification is 42.9, categorized under "Hydrated phosphates, etc. containing hydroxyl or halogen: $(AB)_7(XO_4)_4Z_q \cdot xH_2O$".

4.4. X-Ray Diffraction and Crystallography

4.4.1. Powder X-Ray Diffraction

The observed and calculated X-ray powder diffraction data are presented in Table 2. The seven most intense diffraction lines [d in Å and (I)] are 3.445 (100), 3.108 (72), 4.642 (58), 2.389 (42), 2.997 (36), 4.094 (35), and 2.318 (33). Unit-cell parameters, obtained through indexing and the least-squares refinement of powder diffraction data, indicate a triclinic structure (space group $P-1$, no. 2) with a = 4.7707 (5) Å, b = 8.4869 (7) Å, c = 10.4152 (16) Å, α = 97.070 (10)°, β = 101.030 (10)°, γ = 93.090 (10)°, V = 409.4 (20) Å^3, and Z = 1.

Table 2. The X-ray powder diffraction data (*d* in Å) for zheshengite.

I_{obs}	d_{obs}	I_{calc}	d_{calc}	*h k l*
19	6.10	24	6.0701	0 1 1
6	5.08	6	5.0586	0 0 2
58	**4.642**	43; 40	4.6717; 4.6066	1 0 0; 1 0 −1
23	4.218	9; 17	4.2252; 4.2007	1 −1 0; 0 2 0
35	**4.094**	7; 26; 4	4.0944; 4.0813; 4.0649	0 1 2; 0 2 −1; −1 1 1
18	3.943	4; 13	4.0141; 3.9511	1 1 −1; 1 0 1
13	3.721	7	3.7051	0 2 1
100	**3.445**	71; 100; 84	3.4724; 3.4388; 3.4219	0 2 −2; −1 1 2; 1 1 1
29	3.288	39	3.2883	0 1 −3
72	**3.108**	18; 77; 4; 59; 32	3.1337; 3.1273; 3.0812; 3.0770; 3.0661	1 0 2; −1 2 1; 1 2 −1; 1 −1 2; 1 −2 1
36	**2.997**	3; 72; 52	3.0380; 3.0092; 2.9921	1 0 −3; 1 2 0; 0 1 3
26	2.915	74; 29	2.9251; 2.8895	1 1 −3; 1 2 −2
34	2.806	22; 11; 46; 6	2.8242; 2.8130; 2.8005; 2.7935	0 2 −3; 1 1 2; 0 3 0; −1 1 3
4	2.694	6	2.6944	1 −2 2
14	2.612	10; 16	2.6092; 2.6049	0 3 1; 0 3 −2
15	2.502	20; 4; 25; 10; 6	2.5293; 2.5184; 2.5021; 2.4891; 2.4707	0 0 4; 0 1 −4; 1 −1 3; 1 −3 0; 0 2 3
42	**2.389**	9; 64; 13; 10	2.4001; 2.3829; 2.3817; 2.3773	1 1 −4; 2 0 −1; −1 2 3; 1 3 −1
33	**2.318**	13; 4; 32; 4; 10; 4; 17	2.3358; 2.3234; 2.3199; 2.3149; 2.3131; 2.3023; 2.2865	0 1 4; 1 3 0; 0 3 2; 0 3 −3; 1 1 3; 1 −2 3; −1 1 4
5	2.231	5; 8; 5	2.2298; 2.2208; 2.2129	−2 1 2; −1 3 2; 2 1 −2
12	2.186	5; 5	2.1823; 2.1663	2 0 1; 1 3 1
5	2.122	4; 9; 6	2.1371; 2.1146; 2.1126	1 3 −3; 0 4 −1; 2 −2 0
7	2.074	11	2.0700	1 −1 4
18	2.027	9; 8; 4; 18; 8; 3; 5; 8	2.0316; 2.0311; 2.0234; 2.0230; 2.0187; 2.0092; 2.0071; 2.0006	2 2 −1; 0 1 −5; 0 3 3; 2 −2 1; 0 3 −4; 1 0 −5; 2 2 −2; 1 1 −5
17	1.969	12; 3; 14	1.9763; 1.9741; 1.9535	2 −1 2; 1 −4 0; 1 −4 1
7	1.912	6; 11; 6	1.9113; 1.9029; 1.9004	2 2 −3; 0 4 −3; 1 4 −1
32	1.870	11; 6; 18; 8; 10; 17; 15	1.8859; 1.8758; 1.8740; 1.8735; 1.8666; 1.8589; 1.8541	2 1 −4; 2 −2 2; 2 1 2; 1 4 −2; 1 −4 2; −2 3 1; −2 1 4
9	1.809	3	1.8126	−1 4 2
16	1.791	9; 15; 10; 5	1.7889; 1.7870; 1.7737; 1.7711	1 4 −3; 1 −3 4; 2 3 −1; 2 2 −4
11	1.748	4; 15; 8; 14; 7; 5; 4; 5	1.7615; 1.7508; 1.7477; 1.7448; 1.7368; 1.7345; 1.7331; 1.7194	−1 3 4; 1 2 4; 1 3 3; −1 2 5; 1 −4 3; 1 0 5; 0 2 5; −2 2 4
18	1.687	14; 12; 8; 6; 8; 11; 6; 7; 10; 7; 3	1.7172; 1.7078; 1.7077; 1.6983; 1.6862; 1.6834; 1.6830; 1.6814; 1.6803; 1.6723; 1.6676	1 3 −5; 2 0 −5; 2 3 −3; 1 0 −6; 0 0 6; −2 3 3; 0 4 3; 2 1 3; 0 5 0; −1 4 3; 1 4 −4
12	1.647	3; 18; 5; 11	1.6550; 1.6441; 1.6439; 1.6419	−2 1 5; 0 2 −6; 1 4 2; 2 3 1
14	1.589	10; 6	1.5862; 1.5797	−1 5 1; 2 −1 4
6	1.542	8; 7; 7	1.5433; 1.5330; 1.5245	1 5 0; 2 −4 2; −1 4 4
24	1.501	8; 4; 4; 6; 5; 5; 5; 3; 11	1.5145; 1.5102; 1.5073; 1.4987; 1.4971; 1.4969; 1.4966; 1.4964; 1.4935	−3 1 3; 3 1 0; 1 4 3; 3 −2 0; 2 3 −5; −3 2 2; 0 5 −4; 3 −1 1; 1 0 6
14	1.462	9	1.4661	1 0 −7
9	1.450	8; 4; 11	1.4573; 1.4481; 1.4428	3 2 −1; 3 1 1; 3 1 −4
11	1.407	5; 6; 7; 3; 3; 3; 4; 3; 6	1.4169; 1.4169; 1.4050; 1.4024; 1.3994; 1.3973; 1.3931; 1.3894; 1.3855	3 −1 2; −3 3 1; −2 5 1; 2 −5 1; 0 6 −2; 2 0 5; 0 1 7; −2 4 4; 2 −2 5
6	1.353	3; 6; 6; 3; 3	1.3794; 1.3672; 1.3489; 1.3467; 1.3435	−3 2 4; 0 4 5; 1 −6 2; 1 2 6; 2 5 −1
3	1.327	3; 7	1.3255; 1.3232	3 −1 3; 2 2 −7
15	1.306	5; 4; 4; 3	1.3079; 1.3046; 1.3036; 1.3004	1 6 −3; 0 6 2; 2 −5 3; 3 −4 0
7	1.279	5; 3	1.2806; 1.2506	0 5 −6; 3 −3 3
7	1.247	4; 3	1.2350; 1.2340	0 6 3; 2 5 −5
3	1.212	5	1.2101	−3 2 6
7	1.190	5; 3; 3	1.1914; 1.1909; 1.1831	4 0 −2; −2 4 6; −2 3 7

Lines with *I* ≥ 3 are listed and the seven strongest observed lines are in bold.

4.4.2. Single-Crystal X-Ray Diffraction and Structure Determination

The unit-cell parameters obtained from single-crystal XRD data are shown in Table 3. Structure refinements confirmed the centrosymmetric space group *P*−1 (no. 2). Details of data collection and refinement are in Table 3, while atomic coordinates and site occupancies

are listed in Tables 4 and 5. The crystallographic CIF file and checkCIF report can be found in the supplementary materials.

Table 3. The data collection and structure refinement details for zheshengite.

Crystal Data	
Structural formula	$Pb_4ZnZn_2[(As_{0.680\,(11)}P_{0.320\,(11)})O_4]_2[(P_{0.854\,(10)}P_{0.146\,(10)})O_4]_2(OH)_2$
M_r	1509.27
Crystal system, space group	Triclinic, $P-1$
Temperature (K)	293
a, b, c (Å)	4.7746 (4), 8.4920 (7), 10.4056 (8)
α, β, γ (°)	97.087 (7), 101.060 (7), 92.996 (7)
V (Å^3)	409.66 (6)
Z	1
Radiation type	Mo $K\alpha$
μ (mm^{-1})	48.89
Crystal size (mm)	$0.03 \times 0.02 \times 0.01$
Data collection	
Diffractometer	XtaLAB PRO-007HF
Absorption correction	Multi-scan
T_{min}, T_{max}	0.414, 1.000
No. of measured, independent and observed [$I > 2\sigma(I)$] reflections	3100, 1441, 1315
R_{int}	0.022
$(\sin\theta/\lambda)_{max}$ (Å^{-1})	0.595
Indices range of h, k, l	$-5 < h < 5, -10 < k < 10, -12 < 1 < 12$
Refinement	
$R[F^2 > 2\sigma(F^2)], wR(F^2), S$	0.036, 0.094, 1.12
No. of reflections	1441
No. of parameters	135
No. of restraints	6
$\Delta\rho_{max}, \Delta\rho_{min}$ (e Å^{-3})	3.69, -1.67

Table 4. The atomic coordinates, Wyckoff position, site occupancy, and equivalent isotropic displacement parameters (Å^2) for zheshengite.

Site	Atom	Wyckoff Position	Occupancy	x/a	y/b	z/c	U_{iso}*/U_{eq}
A	Pb1	2i	1	0.64896 (10)	0.48033 (6)	0.83008 (5)	0.0185 (2)
	Pb2	2i	1	0.60078 (11)	0.89548 (6)	0.66164 (5)	0.0224 (2)
^{VI}B	Zn1	1c	1	0.500000	0.500000	0.500000	0.0187 (5)
^{IV}B	Zn2	2i	1	0.8316 (3)	0.87375 (18)	1.11714 (15)	0.0169 (3)
$X1$	P1	2i	0.320 (11)	0.0021 (3)	0.75104 (19)	0.41066 (15)	0.0126 (6)
	As1	2i	0.680 (11)	0.0021 (3)	0.75104 (19)	0.41066 (15)	0.0126 (6)
$X2$	P2	2i	0.854 (10)	1.2593 (5)	0.7787 (3)	0.9363 (3)	0.0132 (10)
	As2	2i	0.146 (10)	1.2593 (5)	0.7787 (3)	0.9363 (3)	0.0132 (10)
	O1	2i	1	1.176 (2)	0.8994 (11)	0.8359 (10)	0.025 (2)
	O2	2i	1	1.5940 (19)	0.7590 (11)	0.9566 (9)	0.020 (2)
	O3	2i	1	1.1111 (19)	0.6098 (12)	0.8839 (10)	0.026 (2)
	O4	2i	1	1.2046 (19)	0.8391 (12)	1.0769 (8)	0.021 (2)
	O5	2i	1	-0.210 (2)	0.7876 (13)	0.2774 (10)	0.030 (2)
	O6	2i	1	0.2416 (18)	0.8997 (11)	0.4749 (9)	0.021 (2)
	O7	2i	1	-0.1932 (19)	0.7101 (11)	0.5172 (9)	0.022 (2)
	O8	2i	1	0.1716 (18)	0.5931 (10)	0.3693 (8)	0.0172 (19)
	O9(OH)	2i	1	0.4146 (18)	0.6166 (10)	0.6645 (9)	0.0177 (19)

Table 5. The anisotropic displacement parameters (in Å^2) for zheshengite.

Site	Atom	U^{11}	U^{22}	U^{33}	U^{12}	U^{13}	U^{23}
A	Pb1	0.0190 (3)	0.0209 (3)	0.0165 (3)	0.0037 (2)	0.0054 (2)	0.0023 (2)
	Pb2	0.0225 (3)	0.0222 (3)	0.0216 (3)	0.0025 (2)	0.0038 (2)	−0.0002 (2)
^{VI}B	Zn1	0.0206 (11)	0.0215 (11)	0.0152 (11)	0.0084 (9)	0.0063 (9)	−0.0006 (9)
^{IV}B	Zn2	0.0165 (8)	0.0203 (8)	0.0145 (8)	0.0038 (6)	0.0059 (6)	0.0001 (6)
$X1$	P1	0.0114 (9)	0.0163 (10)	0.0108 (9)	0.0043 (6)	0.0031 (6)	0.0017 (6)
	As1	0.0114 (9)	0.0163 (10)	0.0108 (9)	0.0043 (6)	0.0031 (6)	0.0017 (6)
$X2$	P2	0.0106 (15)	0.0167 (15)	0.0130 (16)	0.0042 (10)	0.0058 (10)	−0.0024 (11)
	As2	0.0106 (15)	0.0167 (15)	0.0130 (16)	0.0042 (10)	0.0058 (10)	−0.0024 (11)
	O1	0.023 (5)	0.022 (5)	0.031 (6)	0.009 (4)	0.009 (4)	0.002 (4)
	O2	0.015 (5)	0.025 (5)	0.017 (5)	0.003 (4)	0.003 (4)	−0.008 (4)
	O3	0.015 (5)	0.033 (6)	0.033 (6)	0.006 (4)	0.012 (4)	0.005 (5)
	O4	0.016 (4)	0.035 (5)	0.011 (4)	0.005 (4)	0.005 (3)	−0.009 (4)
	O5	0.028 (5)	0.046 (6)	0.018 (5)	0.004 (5)	0.006 (4)	0.013 (5)
	O6	0.011 (4)	0.025 (5)	0.028 (5)	0.009 (4)	0.008 (4)	0.000 (4)
	O7	0.020 (5)	0.026 (5)	0.023 (5)	0.012 (4)	0.006 (4)	0.008 (4)
	O8	0.015 (5)	0.022 (5)	0.016 (5)	0.005 (4)	0.009 (4)	0.000 (4)
	O9(OH)	0.016 (5)	0.018 (5)	0.017 (5)	0.003 (4)	0.003 (4)	−0.002 (4)

Dongchuanite group minerals form an isomorphous series, with their structures projected along [100] as illustrated in Figure 3a. The framework comprises two distinct types of heteropolyhedral chains aligned along [100] (Figure 3a,b). These chains, connected by corner-sharing [$^{IV}BO_4$] and [$X1O_4$] tetrahedra, form layers parallel to the (011) plane (Figure 3b). Chain A consists of corner-sharing [$^{IV}BO_4$] and [$X2O_4$] tetrahedra, with each tetrahedron three-connected within the chain. Chain B features alternating [$^{VI}BO_4(OH)_2$] octahedra and paired corner-linked [$X1O_4$] tetrahedra. Pb atoms occupy two independent interlayer sites.
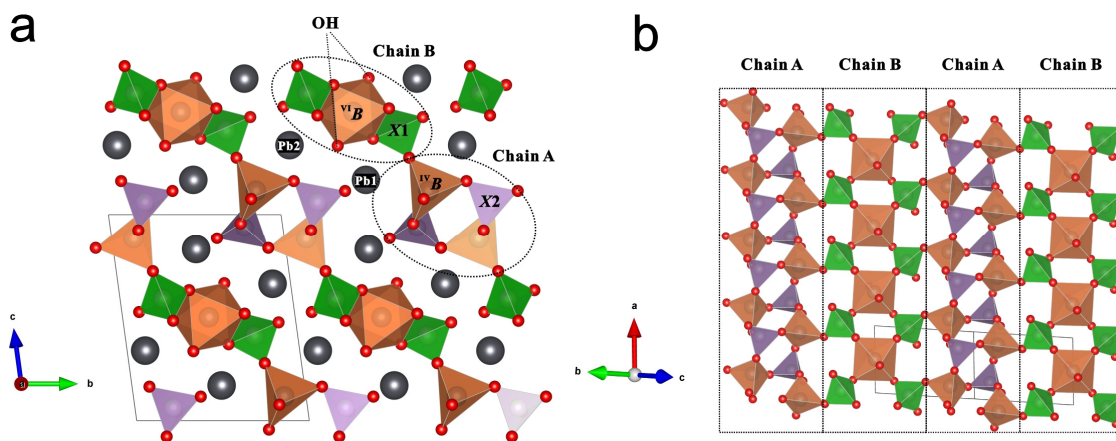

Figure 3. (**a**) The projection of the dongchuanite group mineral structure along [100], illustrating the isomorphous series and spatial arrangement of heteropolyhedral chains. (**b**) The detailed view of heteropolyhedral chains A and B aligned along [100], showing corner-sharing [$^{IV}BO_4$] and [$X1O_4$] tetrahedra that form layers parallel to the (011) plane. The crystal structure diagram was generated using Vesta software [10].

The bond lengths of zheshengite are given in Table 6. Chemical composition and structural refinement data for zheshengite reveal that Zn predominantly occupies both ^{VI}B and ^{IV}B sites. The interatomic distances at the ^{VI}B site indicate six bonds in the range of 1.9–2.2 Å, with an average bond length of 2.110 Å. At the ^{IV}B site, four bonds range from 1.93 to 1.94 Å, averaging 1.938 Å. Site occupancy refinements and bond valence sums (Table 7) indicate that the $X1$ and $X2$ sites are mainly occupied by As and P, respectively.

The scattering power observed at the *X1* and *X2* sites falls between that expected for "pure P" and "pure As," suggesting partial occupancy by both elements. Subsequent refinements indicate that *X1* is primarily occupied by As, with a composition of 0.680 (11) As and 0.320 (11) P, while *X2* is predominantly P, with 0.854 (10) P and 0.146 (10) As. Due to the larger atomic radius of As relative to P, *X1* contains more As than the *X2* site, and the average *X1*–O bond length (1.640 Å) is greater than that of *X2*–O (1.568 Å). Both Pb sites exhibit asymmetrical coordination typical of Pb^{2+}, influenced by the stereochemically active lone-pair electrons of the $6s^2$ configuration. Pb1 forms four bonds between 2.33 and 2.61 Å, along with three elongated bonds ranging from 2.96 to 3.06 Å. Pb2, on the other hand, forms four bonds in the range of 2.33 to 2.54 Å, supplemented by two extended bonds at 2.96 and 3.98 Å.

Table 6. The selected bond lengths (Å) for zheshengite.

Pb1—O2 [i]	2.614 (9)	Pb2—O1	2.983 (10)
Pb1—O3	2.348 (9)	Pb2—O1 [i]	2.968 (10)
Pb1—O3 [i]	2.968 (9)	Pb2—O6 [v]	2.548 (9)
Pb1—O4 [ii]	3.061 (10)	Pb2—O6	2.337 (9)
Pb1—O5 [iii]	2.966 (11)	Pb2—O7 [vi]	2.419 (9)
Pb1—O8 [iv]	2.417 (8)	Pb2—O9	2.492 (9)
Pb1—O9	2.334 (8)	**<Pb2–O>**	**2.625**
<Pb1–O>	**2.673**		
Zn1—O7 [vi]	2.215 (10)	Zn2—O1 [vii]	1.932 (9)
Zn1—O7 [iii]	2.215 (10)	Zn2—O2 [i]	1.945 (9)
Zn1—O8 [iv]	2.124 (8)	Zn2—O4	1.935 (9)
Zn1—O8	2.124 (8)	Zn2—O5 [viii]	1.941 (10)
Zn1—O9 [iv]	1.992 (9)	**<Zn2–O>**	**1.938**
Zn1—O9	1.992 (9)		
<Zn1–O>	**2.110**		
X1–O5	1.626 (10)	X2–O1	1.565 (10)
X1–O6	1.642 (10)	X1–O2	1.591 (9)
X1–O7	1.636 (9)	X1–O3	1.552 (10)
X1–O8	1.657 (8)	X1–O4	1.565 (9)
<X1–O>	**1.640**	**<X1–O>**	**1.568**

Symmetry codes: [i] $x - 1, y, z$; [ii] $-x + 2, -y+1, -z + 2$; [iii] $-x, -y + 1, -z + 1$; [iv] $-x + 1, -y + 1, -z + 1$; [v] $-x + 1, -y + 2, -z + 1$; [vi] $x + 1, y, z$; [vii] $-x + 2, -y + 2, -z + 2$; [viii] $x + 1, y, z + 1$.

Table 7. The bond valence sum for zheshengite.

	Pb1	Pb2	Zn1	Zn2	X1	X2	H9	O Sum
O1		0.12 0.12		0.52		1.25		**2.01**
O2	0.27			0.51		1.17		**1.95**
O3	0.49 0.12					1.29	0.13	**2.03**
O4	0.10			0.52		1.26		**1.88**
O5	0.12			0.51	1.33			**1.96**
O6		0.50 0.31			1.27			**2.08**
O7		0.42	0.25 × 2 ↓		1.29			**1.96**
O8	0.42		0.32 × 2 ↓		1.22			**1.96**
O9 (OH)	0.50	0.35	0.45 × 2 ↓				0.87	**2.17**
Sum	**2.02**	**1.82**	**2.04**	**2.06**	**5.11**	**4.97**	**1.00**	

Note: The BVS is the calculated bond valences with the ECoN21 program [27] with the equation $S = \exp[R_0 - d_0)/b]$ [28]. The occupancies of *X1* site are $0.680P^{5+} + 0.320As^{5+}$; the occupancies of *X2* site are $0.854P^{5+} + 0.146As^{5+}$. Hydrogen-bond valences are based on O-O bond lengths [29]. The distance between O3 and O9 is 2.945(15) Å. In the hydrogen-bonding system, O9 acts as the donor with a bond valence parameter of 0.87, while O3 serves as the acceptor with a bond valence parameter of 0.13. The downward arrows (e.g., "× 2 ↓") indicate contributions from two equivalent bonds or interactions.

5. Discussion

5.1. Relationship to Other Mineral Species

To date, alongside zheshengite, the dongchuanite group comprises three other minerals, including dongchuanite, cuprodongchuanite, and cuprozheshengite. The general formula of dongchuanite group minerals is $A_4{}^{VI}B^{IV}B_2(X1O_4)_2(X2O_4)_2(OH)_2$ (Table 8). In this formula, *A* represents an interlayer cation, primarily Pb. *B* represents transition metals with two crystallographic positions: ${}^{IV}B$, which has tetrahedral coordination occupied by Zn, and ${}^{VI}B$, which has octahedral coordination, primarily Zn or Cu. Both *X* sites (*X1* and *X2*) are cations with tetrahedral coordination, primarily occupied by P or As. Zheshengite, with the ideal formula $Pb_4ZnZn_2(AsO_4)_2(PO_4)_2(OH)_2$, is the Zn analog of cuprozheshengite and shows an ordered distribution of As and P at the *X1* and *X2* sites. When high-quality structural data are available for occupancy refinement, these minerals should be distinguished based on the structural refinement results of the *X1* and *X2* sites, demonstrating the predominant occupancy of P and As at these sites. However, when only EPMA data are available, the minerals of the isomorphous series can be distinguished using the As: P ratio determined from quantitative chemical analyses. Specifically, minerals with a P: As ratio greater than 3: 1 are identified as dongchuanite (or cuprodongchuanite), those with a P: As ratio less than 1: 3 are classified as the unnamed As-rich phase, and those with intermediate ratios are identified as zheshengite (or cuprozheshengite) (Figure 4).

Table 8. Members and potential members of cuprozheshengite isomorphous minerals ($A_4{}^{VI}B^{IV}B_2(X1O_4)_2(X2O_4)_2(OH)_2$).

| ${}^{VI}B$	X1 = X2 = P	X1 = As, X2 = P	X1 = X2 = As
Zn	Dongchuanite (IMA2021-058) $Pb_4{}^{VI}Zn^{IV}Zn_2(PO_4)_2(PO_4)_2(OH)_2$	Zheshengite (IMA2022-011) $Pb_4{}^{VI}Zn^{IV}Zn_2(AsO_4)_2(PO_4)_2(OH)_2$	Full As analog of dongchuanite (Potential) $Pb_4{}^{VI}Zn^{IV}Zn_2(AsO_4)_2(AsO_4)_2(OH)_2$
Cu	Cuprodongchuanite (IMA2021-065) $Pb_4{}^{VI}Cu^{IV}Zn_2(PO_4)_2(PO_4)_2(OH)_2$	Cuprozheshengite (IMA2022-095a) $Pb_4{}^{VI}Cu^{IV}Zn_2(AsO_4)_2(PO_4)_2(OH)_2$	Full As analog of cuprodongchuanite (Potential) $Pb_4{}^{VI}Cu^{IV}Zn_2(AsO_4)_2(AsO_4)_2(OH)_2$
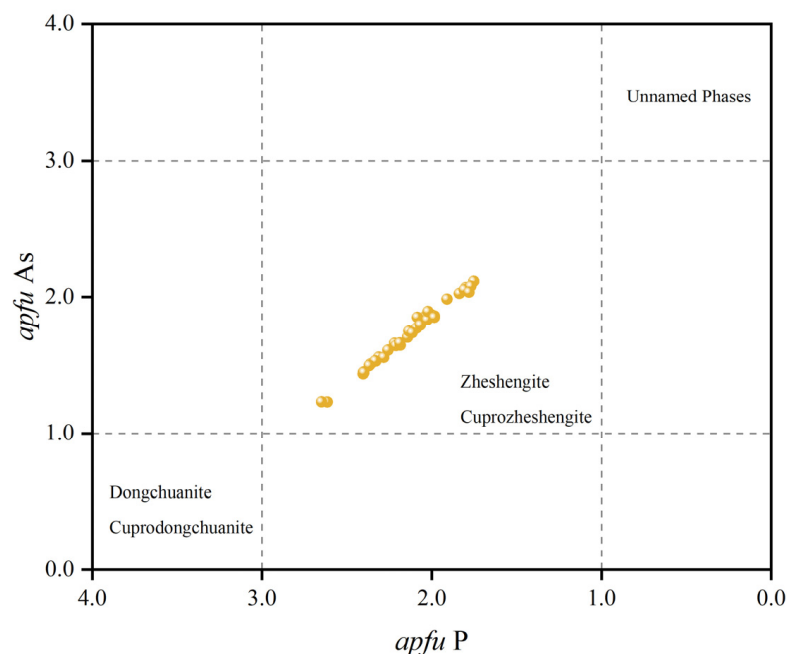
Figure 4. Classification of dongchuanite group minerals based on EPMA data, with a scatter diagram showing apfu P and As values calculated from thirty-nine EPMA data of zheshengite.

5.2. Elemental Contributions from Primary Minerals to the Formation of Zheshengite

Zheshengite is found in cavities and fractures formed after the weathering of primary minerals and is closely associated with hemimorphite, an indicator mineral of supergene processes [30], indicating that zheshengite is also a supergene mineral. The major elements in its composition, including Pb, Zn, As, and P, are derived from primary minerals (Figure 5). Specifically, galena (PbS) provides Pb, sphalerite (ZnS) supplies Zn, and tennantite-(Zn) ($Cu_6(Cu_4Zn_2)As_4S_{12}S$) contributes Cu, Zn, and As. Additionally, the dolomite host rock contains abundant apatite, which creates a P-rich environment in the system. The formation of dongchuanite group minerals, characterized by a series of As–P isomorphic substitutions, is closely linked to the widespread occurrence of tennantite-(Zn) in the deposit, which supplies a sufficient amount of As.
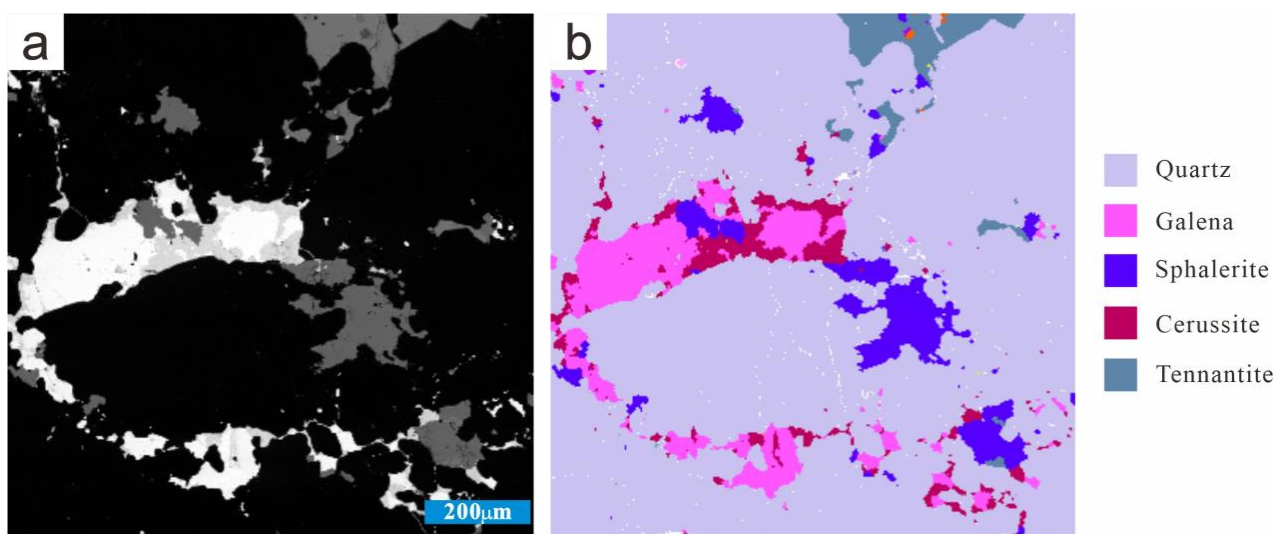
Figure 5. BSE image and mineral mapping of a rock thin section containing primary minerals from the type locality of zheshengite: (**a**) BSE image, showing black, grey, and white contrasts for different minerals; (**b**) mineral mapping with false colors distinguishing various minerals.

5.3. The Influence of As–P Isomorphic Substitution on Unit-Cell Parameters

The larger ionic radius of As compared to P suggests that the isomorphic substitution of P by As at tetrahedral sites likely alters unit-cell parameters, as shown in studies on philipsburgite [31] and goldhillite [24].

In Table 9, we summarize the cell parameters of 13 dongchuanite group minerals. The unit-cell parameter *a* is mainly within the range of 4.7311 Å to 4.8161 Å, *b* ranges from 8.4864 Å to 8.5902 Å, and *c* spans from 10.2723 Å to 10.4130 Å. The unit-cell volume *V* varies between 400.63 Å^3 and 417.29 Å^3.

By analyzing the As/(As + P) ratio obtained through structural refinement (Figure 6), we observed a linear correlation between this ratio and the unit-cell parameters *a* and *V*, with goodness-of-fit values of $R^2 = 0.917$ for *a* and $R^2 = 0.866$ for *V*. This strong correlation suggests that the increase in As content significantly affects the parameters *a* and *V*. In contrast, the substitution of As for P has a less significant effect on parameters *b* and *c*, as evidenced by lower R^2 values of 0.470 for *b* and 0.316 for *c*. This indicates that the variations in *a* and *V* may reflect the degree of As substitution in the minerals of the dongchuanite group.

Furthermore, the extent of As content influences the naming and classification within the dongchuanite group [9,10]. Consequently, the values of *a* and *V* could serve as useful criteria for distinguishing and identifying minerals in this group. These parameters provide insight into the extent of arsenic substitution and may aid in the mineral identification process within the dongchuanite group.

Table 9. The occupancy of the *X* site, the As/(As + P) ratio, and cell parameters of dongchuanite group minerals.

| No.	Species	Occupancy of *X*1 Site	Occupancy of *X*2 Site	As/As+P	*a*	*b*	*c*	*α*	*β*	*γ*	*V*
1	Dongchuangite	0.64 (2) P + 0.364 (19) As	1.00P	0.18	4.7620 (10)	8.507 (2)	10.3641 (19)	97.110 (17)	101.465 (17)	92.273 (18)	407.44 (15)
2	Cuprodongchuanite	0.85 (2) P + 0.15 (2) As	1.00P	0.08	4.7311 (7)	8.5054 (15)	10.2723 (19)	97.172 (15)	101.885 (14)	91.814 (13)	400.63 (12)
3	Cuprodongchuanite	0.86 (2) P + 0.142 (17) As	1.00P	0.07	4.7359 (5)	8.4995 (9)	10.2922 (13)	97.247 (10)	102.059 (10)	91.758 (8)	401.22 (8)
4	Cuprodongchuanite	0.63 (3) P + 0.37 (2) As	1.00P	0.19	4.7608 (14)	8.5119 (18)	10.3269 (14)	97.371 (15)	101.80 (2)	91.99 (2)	405.45 (16)
5	Zheshengite	0.31 (2) P + 0.686 (12) As	0.86 (2) P + 0.144 (12) As	0.42	4.7727 (4)	8.4864 (6)	10.4053 (7)	97.083 (6)	101.002 (7)	93.072 (7)	409.25 (5)
6	Zheshengite	0.32 (2) P + 0.678 (17) As	0.82 (2) P + 0.178 (16) As	0.43	4.7697 (7)	8.4948 (12)	10.4036 (9)	97.161 (10)	101.047 (10)	92.982 (12)	409.24 (9)
7	Zheshengite	0.29 (2) P + 0.713 (17) As	0.81 (2) P + 0.187 (16) As	0.45	4.7774 (4)	8.5027 (6)	10.4130 (7)	97.151 (7)	100.987 (7)	92.996 (7)	410.75 (6)
8	Cuprozheshengite	0.29 (2) P + 0.705 (19) As	0.66 (2) P + 0.340 (19) As	0.52	4.8005 (15)	8.550 (2)	10.4047 (18)	97.268 (17)	101.84 (2)	91.68 (2)	413.91 (18)
9	Cuprozheshengite	0.40 (2) P + 0.604 (16) As	0.78 (2) P + 0.224 (16) As	0.41	4.7660 (10)	8.5124 (12)	10.3115 (16)	97.125 (13)	101.714 (16)	91.626 (14)	405.84 (12)
10	Cuprozheshengite	0.19 (2) P + 0.810 (18) As	0.55 (2) P + 0.451 (18) As	0.63	4.8161 (9)	8.5902 (10)	10.4056 (11)	97.448 (9)	101.744 (13)	91.545 (12)	417.29 (10)
11	Cuprozheshengite	0.236 (19) P + 0.764 (11) As	0.620 (19) P + 0.382 (11) As	0.57	4.7977 (8)	8.5789 (8)	10.3855 (9)	97.270 (8)	101.902 (12)	91.495 (11)	414.30 (9)
12	Cuprozheshengite	0.28 (2) P + 0.719 (15) As	0.80 (2) P + 0.197 (15) As	0.46	4.7860 (6)	8.5169 (10)	10.3184 (13)	97.253 (10)	101.925 (12)	91.526 (11)	407.62 (9)
13	Cuprozheshengite	0.36 (2) P + 0.64 (2) As	0.91 (1) P + 0.09 (1) As	0.37	4.7650 (10)	8.520 (2)	10.349 (2)	97.23 (3)	101.81 (3)	91.72 (3)	407.31 (16)
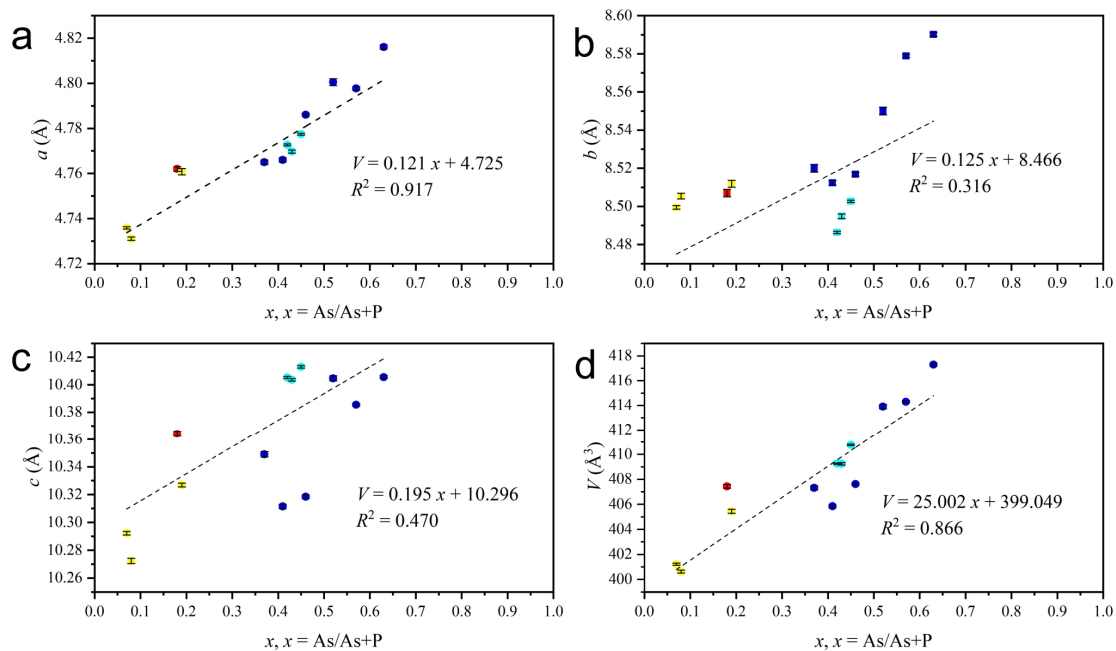
Figure 6. Relationship between the As/(As + P) ratio and unit-cell parameters (*a*, *b*, *c*, and *V*) in dongchuanite group minerals. The red points represent dongchuanite, the yellow points represent cuprodongchuanite, the dark blue points represent cuprozheshengite, and the light blue points represent zheshengite: (**a**) The cell parameter *a* shows a strong linear correlation with the As/(As + P) ratio. (**b**) The cell parameter *b* shows a weaker linear correlation with the As/(As + P) ratio. (**c**) The cell parameter *c* shows a weaker linear correlation with the As/(As + P) ratio. (**d**) The unit-cell volume *V* exhibits a strong linear correlation with the As/(As + P) ratio.

6. Conclusions

In summary, zhengshengite, a member of the dongchuanite mineral group, is characterized by Zn occupancy at the both *B* sites, with As and P preferentially occupying the *X*1 and *X*2 sites, respectively. For dongchuanite group minerals, the isomorphous substitution

of P by As was found to significantly contribute to the expansion of cell parameter *a* and the unit-cell volume *V*.

References

1. Li, G.; Sun, N.; Xue, Y. Establishment of the dongchuanite group, CNMNC Newsletter 74. *Miner. Mag.* **2023**, *87*, 787. [CrossRef]
2. Lacalle, R.G.; Bernal, M.P.; Álvarez-Robles, M.; Clemente, R. Phytostabilization of soils contaminated with As, Cd, Cu, Pb and Zn: Physicochemical, toxicological and biological evaluations. *Soil Environ. Health* **2023**, *1*, 100014. [CrossRef]
3. Kumpiene, J.; Guerri, G.; Landi, L.; Pietramellara, G.; Nannipieri, P.; Renella, G. Microbial biomass, respiration and enzyme activities after in situ aided phytostabilization of a Pb- and Cu-contaminated soil. *Ecotoxicol. Environ. Saf.* **2009**, *72*, 115–119. [CrossRef]
4. Pereira, P.; Bogunovic, I.; Munoz-Rojas, M.; Brevik, E.C. Soil ecosystem services, sustainability, valuation and management. *Curr. Opin. Environ. Sci. Health* **2018**, *5*, 7–13. [CrossRef]
5. Kocourkova-Vikova, E.; Loun, J.; Sracek, O.; Houzar, S.; Filip, J. Secondary arsenic minerals and arsenic mobility in a historical waste rock pile at Kank near Kutna Hora, Czech Republic. *Miner. Petrol.* **2015**, *109*, 17–33. [CrossRef]
6. Liang, X.; Lin, X.; Wei, G.; Ma, L.; He, H.; Carballal, D.S.; Zhu, J.; Zhu, R.; Leeuw, N.D. Competitive adsorption geometries for the arsenate As(V) and phosphate P(V) oxyanions on magnetite surfaces: Experiments and theory. *Am. Miner.* **2021**, *106*, 374–388. [CrossRef]
7. Xing, S.; Guo, H.; Zhang, L.; Wang, Z.; Sun, X. Silicate weathering contributed to arsenic enrichment in geotherm-affected groundwater in Pliocene aquifers of the Guide basin, China. *J. Hydrol.* **2022**, *606*, 127444. [CrossRef]
8. Kunhikrishnan, A.; Choppala, G.; Seshadri, B.; Wijesekara, H.; Bolan, N.S.; Mbene, K.; Kim, W.I. Impact of wastewater derived dissolved organic carbon on reduction, mobility, and bioavailability of As(V) and Cr(VI) in contaminated soils. *J. Environ. Manag.* **2017**, *186*, 183–191. [CrossRef]
9. Li, G.; Sun, N.; Shen, H.; Xue, Y.; Hao, J.; de Fourestier, J. Dongchuanite, a new phosphate mineral with a new structure, from Dongchuan copper mine, Yunnan Province, China. *Miner. Mag.* **2023**, *87*, 611–618. [CrossRef]
10. Sun, N.; Grey, I.E.; Li, G.; Rewitzer, C.; Xue, Y.; Mumme, W.G.; Shen, H.; Hao, J.; MacRae, C.M.; Riboldi-Tunnicliffe, A.; et al. The new mineral cuprozhesengite, $Pb_4CuZn_2(AsO_4)_2(PO_4)_2(OH)_2$, from Yunnan, China, with site-selective As-P substitution. *Am. Miner.* **2024**, *109*, 1248–1257. [CrossRef]
11. Cao, J. Mint Metal Mining and Minting in Sichuan (1700–1900): Effects on the Regional Economy and Society. Ph.D. Thesis, Universität Tübingen, Tübingen, Germany, 2012.
12. Kim, N.; Yang, Y. The Jinniu mines and the confusions of Qing sources on silver mining. *Artefact* **2018**, *8*, 8. [CrossRef]
13. Zhao, X.; Zhou, M.; Li, J.; Sun, M.; Gao, J.; Sun, W.; Yang, J. Late Paleoproterozoic to early Mesoproterozoic Dongchuan Group in Yunnan, SW China: Implications for tectonic evolution of the Yangtze block. *Precambrian Res.* **2010**, *182*, 57–69. [CrossRef]
14. Ma, Z.; Li, G.; Chukanov, N.V.; Poirier, G.; Shi, N. Tangdanite, a new mineral species from the Yunnan province, china and the discreditation of 'clinotyrolite'. *Miner. Mag.* **2014**, *78*, 559–570. [CrossRef]
15. Zhao, X.; Zhou, M.; Hitzman, M.W.; Li, J.; Bennett, M.; Meighan, C.; Anderson, E. Late Paleoproterozoic to Early Mesoproterozoic Tangdan Sedimentary Rock-Hosted Strata-bound Copper Deposit, Yunnan Province, Southwest China. *Econ. Geol.* **2012**, *107*, 357–375. [CrossRef]
16. Laugier, J.; Bochu, B. *CHECKCELL—A Software Performing Automatic Cell/Space Group Determination*; Collaborative Computational Project Number 14 (CCP14); Laboratoire des Matériaux et du Génie Physique de l' Ecole Supérieure de Physique de Grenoble (INPG): Grenoble, France, 2000.

17. Momma, K.; Izumi, F. VESTA 3 for three-dimensional visualization of crystal, volumetric and morphology data. *J. Appl. Crystallogr.* **2011**, *44*, 1272–1276. [CrossRef]

18. Dolomanov, O.V.; Bourhis, L.J.; Gildea, R.J.; Howard, J.; Puschmann, H. Olex2: A complete structure solution, refinement and analysis program. *J. Appl. Crystallogr.* **2010**, *42*, 339–341. [CrossRef]

19. Sheldrick, G.M. Crystal structure refinement with shelxl. *Acta Crystallogr. C Struct. Chem.* **2015**, *71*, 3–8. [CrossRef] [PubMed]

20. Mandarino, J.A. The Gladstone-Dale relationship: Part IV. The compatibility concept and its application. *Can. Miner.* **1981**, *19*, 441–450.

21. Hawthorne, F.C.; Cooper, M.A.; Abdu, Y.A.; Ball, N.A.; Back, M.E.; Tait, K.T. Davidlloydite, ideally $Zn_3(AsO_4)_2(H_2O)_4$, a new arsenate mineral from the Tsumeb mine, Otjikoto (Oshikoto) region, Namibia: Description and crystal structure. *Miner. Mag.* **2012**, *76*, 45–57. [CrossRef]

22. Frost, R.L.; Martens, W.N.; Williams, P.A. Raman spectroscopy of the phase-related basic copper arsenate minerals olivenite, cornwallite, cornubite and clinoclase. *J. Raman Spectrosc.* **2002**, *33*, 475–484. [CrossRef]

23. Ciesielczuk, J.; Janeczek, J.; Dulski, M.; Krzykawski, T. Pseudomalachite–cornwallite and kipushite–philipsburgite solid solutions: Chemical composition and Raman spectroscopy. *Eur. J. Miner.* **2016**, *28*, 555–569. [CrossRef]

24. Ismagilova, R.; Rieck, B.; Kampf, A.; Giester, G.; Zhitova, E.; Lengauer, C.; Krivovichev, S.V.; Zolotarev, A.A.; Ciesielczuk, J.; Mikhailova, J.A.; et al. Goldhillite, $Cu_5Zn(AsO_4)_2(OH)_6 \cdot H_2O$, a new mineral species, and redefinition of philipsburgite, $Cu_5Zn[(AsO_4)(PO_4)](OH)_6 \cdot H_2O$, as an As–P ordered species. *Miner. Mag.* **2022**, *86*, 436–446. [CrossRef]

25. Farmer, C.V. *The Infrared Spectra of Minerals*; Mineralogical Society Monograph 4; The Mineralogical Society: London, UK, 1974; 539p.

26. Grey, I.E.; Keck, E.; Kampf, A.R.; Macrae, C.M.; Glenn, A.M.; Price, J.R. Wilhelmgümbelite, $[ZnFe^{2+}Fe_3^{3+}(PO_4)_3(OH)_4(H_2O)_5] \cdot 2H_2O$, a new schoonerite-related mineral from the Hagendorf süd pegmatite, Bavaria. *Miner. Mag.* **2017**, *81*, 287–296. [CrossRef]

27. Ilinca, G. Charge Distribution and Bond Valence Sum Analysis of Sulfosalts—The ECoN21 Computer Program. *Minerals* **2022**, *12*, 924. [CrossRef]

28. Brown, I.D. Predicting bond lengths in inorganic crystals. *Acta Crystallogr. Sect. B Struct. Sci.* **1977**, *33*, 1305–1310. [CrossRef]

29. Brown, I.D.; Altermatt, D. Bond-valence parameters obtained from a systematic analysis of the inorganic crystal structure database. *Acta Crystallogr. Sect. B Struct. Sci.* **1985**, *41*, 244–247. [CrossRef]

30. Bouabdellah, M.; Boukirou, W.; Potra, A.; Melchiorre, E.; Bouzahzah, H.; Yans, J.; Zaid, K.; Idbaroud, M.; Poot, J.; Dekoninck, A.; et al. Origin of the Moroccan Touissit-Bou Beker and Jbel Bou Dahar Supergene Non-Sulfide Biomineralization and Its Relevance to Microbiological Activity, Late Miocene Uplift and Climate Changes. *Minerals* **2021**, *11*, 401. [CrossRef]

31. Shirose, Y.; Uehara, S. Philipsburgite from the Yamato mine, Yamaguchi Prefecture, Japan. *J. Miner. Petrol. Sci.* **2011**, *106*, 153–157. [CrossRef]